111(A) - 2.

PROCEEDINGS

REGIONAL SEMINAR ON COASTAL & OFFSHORE ENGINEERING

"Prospects of the Coastal and Offshore Engineering in the 21st Century"

December 9-11, 1991

PANTAI PRIMULA HOTEL
KUALA TERENGGANU, MALAYSIA

Jointly organised by:

Coastal and Offshore Engineering Institute
Faculty of Chemical & Natural Resources Engineering
UNIVERSITI TEKNOLOGI MALAYSIA.

PETRONAS RESEARCH INSTITUTE, MALAYSIA.

PERFORATED WELLBORE STABILITY

by

Dr Ariffin Samsuri
Petroleum Engineering Department
University of Technology Malaysia

ABSTRACT

This paper presents the results of a study into the mechanical stability of perforated wellbore and the factors which affect it. Physical models of the main factors associated with perforated wellbore were generated and exposed to various load regimes and conclusions were drawn with respect to optimising the stability and therefore the productivity of the perforated well. The results show that the failure depends on the pressure differential between wellbore and formation, the perforation length, shot density, phasing angle and pattern.

INTRODUCTION

The objective of a perforation is to provide a good and effective communication channel between the cased wellbore and the productive zone to enchance the optimum perforated well productivity. Theoretically, perforated well productivity can be equal to or higher than the openhole capacity, but in practice, the perforated well productivity is less than predicted. This reflects the assumptions and simulated perforating and perforations conditions employed in the theoretical models. Perforation and perforated wellbore collapse during creation or subsequent production life may be one of the many inter-related design factors incorrectly modelled.

Many studies have been conducted on charge and gun performance,[1-3] casing damage,[4-5] perforating techniques and conditions,[6-9] and on the nature of flow around and into the perforations.[10-13] The problems of perforation stability have, in the main, concentrated on the effects of high flow rates through perforations and the stability of perforations in friable and weakly consolidated formations.[14-21] However, the interaction between the wellbore and the perforations as a structure within the rock mass, and the material properties of the rock mass must be considered in the design of a perforating system for the perforated wellbore.

The wellbore and the perforations will redistribute the earth stresses within the rock and cause local deformation. If the ultimate strain is not exceeded, the rock will deform elastically. However, if the ultimate is exceeded, the overstressed region will be deformed plastically and may collapse. Operationally, the majority of perforations within the perforated wellbore system are created by shaped charges which generate very high pressures in excess of the strength of the formation. This develops a compacted zone around the perforation tunnel and wellbore. The mechanical stability of the perforated wellbore may be compromised by the structure created around the wellbore by perforating, and may lead to collapse of the perforations and the wellbore during creation or subsequent production life, resulting in lower perforated well productivity.

THE MODELS

The physical models consisted of two types: blocks and thick hollow cylinders. The blocks were sandstone with laboratory tensile and uniaxial compressive strengths of 3.0 MN/m and 29.0 MN/m , respectively. The dimensions were 457 mm by 305 mm by 305 mm, with a 127 mm diameter hole cored in them to represent a wellbore. They were then split along the axis of the hole to provide two half boreholes.

To represent the casing, a steel pipe of 102 mm inside diameter and 114 mm outside diameter was cut to the correct length. The section of steel pipe was then cut into two halves through the centre and trimmed to the exact dimensions to fit exactly to the block. Once the steel pipes were of the correct dimension, the 12 mm diameter holes were then drilled through the wall in accordance with the particular shot density, phasing angle, spacing and pattern of the block to be cemented. The perforated steel pipe was then cemented to the corresponding block using Fondu cement with 3 to 1 cement water ratio. The cemented block was left over night to allow the cement to set under load. The holes of 12 mm diameter were drilled right through the cement into the sandstone block to the desired depth to represent the perforations.

Fourteen blocks were tested under uniaxial compression within a servo-controlled stiff testing machine. A plot of axial load against axial deformation was produced to indicate the onset of failure of the block. A two arm caliper was devised to measure the diametral deformation of the perforation. Three were made and they consisted of two steel arms braised to a block of steel. A strain gauge on the arm measured the deflection, and all the calipers were calibrated regularly. They were oriented within the perforations to measure vertical displacement as it was expected that failure would initiate at the sides of the perforations. The dimensions of the perforations and of the block precluded development of an instrument to measure the horizontal deformation and the depth of the fractures produced.

The blocks were then loaded at constant rate of 0.7 MN/m /s until they failed. Measurements were taken at regular load increments and the development of fractures within the wellbore was photographed. After failure, the debris from the block was collected for sieve analysis and the blocks were cut along the perforation tunnel axis for inspection of the perforation failure mode and fracture orientation. A model of the perforation was then produced in modelling clay.

The hollow cylinder models were 110 mm long, 55 mm diameter with a 25 mm diameter hole located coaxially within the core. 5 mm perforations were drilled through the cylinder walls at different shot densities , phasing angles and patterns. The cylinders were confined in a triaxial cell which was located within the stiff testing machine. Both confining stress and axial load were applied by servo-controlled hydraulics. Small calipers were devised to measure diametral deformation of the perforations. A hollow cylindrical platen was produced and used at the bottom of the assembly through which the electrical leads of the strain gauge were brought out the hollow cylinder and to collect debris produced during the loading process. 36 specimens were tested to failure at different confining pressures of 50, 100 and 150 bar. At each succesive axial load increment, the extent of the fractures within the cylinders was estimated visually, through the hollow cylindrical platen. After failure, the debris was collected and sieved. The cylinders were cut axially, the extent of the fractures logged, and a net produced of their orientation around the wellbore.

RESULTS

In general, the results showed that there is a complex interaction between the redistributed stresses around the wellbore and the perforation. The perforation diameter decreases with increasing applied stress and the perforation tunnel was seen to deform and spall at the sides. The deformation mechanism appears similar to wellbore breakout. The top and bottom sections of the perforations had deformed but had not failed.

The failure depends on the pressure differential between wellbore and formation, the perforation length, shot density, phasing angle and pattern. A local fracture is initiated at the centre of both side walls of the perforation entrance hole or of the cement-rock interface. As the load increases further, the fracture propagates along the perforation tunnel until massive failure of the model. Failure will occur along any pre-existing weak planes which intersect the perforation tunnels. The debris produced was found by sieve analysis to be oversized 500 microns. The debris created within the rock adjacent to the perforation tunnel surface will contribute to any possible formation and perforation plugging. More stable structure produce less debris. Table 1 summarises the results of the modelling.

Perforated Wellbore Stability

The stability is the overall effect produced by the interaction of the perforation and wellbore geometries with the rock stresses and in this study, was simply related to the failure load of the structure. In general, the perforated wellbore stability depends on the pressure differential, perforation length, shot density, phasing angle and pattern.

The results show the perforated wellbore stability decreases as the pressure differential, length, and shot density increase, and phasing angle decreases depending on the pattern.

As the length and/or shot density increases, the stability decreases in that the interaction between the individual perforations increases the redistributed

TABLE 1

SUMMARY OF THE RESULTS

PARAMETER	INFLUENCE				
	PERFORATED WELLBORE STABILITY	PERFORATION DIAMETER DEFORMATION	MODE AND ORIENTATION OF FRACTURE	MASS OF DEBRIS PRODUCED	DEBRIS SIZE DISTRIBUTION (> 500cm)
Perforation Length	1	1	X	2	2
Shot Density	1	1	X	2	2
Phasing Angle	2	2	X	1	1
Inline Pattern	Weakest	Smallest	X	Highest	Highest
Inplane Pattern	Medium	Medium	X	Medium	Medium
Spiral Pattern	Stronger	Largest	X	Lowest	Lowest
Rock Type (Strength)	2	X	X	1	1
Confining Pressure	2		X	1	2

NOTE:

1 = Indicates that as the parameter increases the influence decreases.
2 = Indicates that as the parameter increases as the influence increases.
X = Indicates that the parameter has come influence.

stresses. Increasing the perforation length will reduce the amount of rock mass within the system, therefore more load must be carried by the surrounding rock, resulting in redistributed stress and a reduction of rock mass strength. Fig. (1) shows a typical plot of pressure differential at failure for various perforation length. The stable region becomes smaller as the perforation length increases.

The perforated wellbore stability decreases as the shot density increases, even though the perforation length decreases. This may be due to stress redistribution, since the stress and strain around the system will increase as the shot density increases. Increasing shot density by definition will reduce the amount of rock matrix within the perforated wellbore system, therefore more load must be carried by the surrounding rock, resulting in a reduction of rock mass strength and also, there are greater stress concentration in the rock between perforation tunnels. Fig. (2) shows a typical plot of pressure differential at failure for various shot densities. The area of stable pressure differential becomes smaller as the shot density increases.

The shot phasing angle and pattern affect the stability. The perforated wellbore stability increases as the phasing angle increases, depending on the pattern, as shown in Fig. (3). An inline pattern of 0 phasing angle produced the least stable configuration. An inplane pattern, irrespective of the phasing, produced a more stable configuration and a spiral pattern, of various shot phasing angle produced the most stable configuration. This is because in a spiral pattern, the perforations are in a line inclined to the effective overburden load, resulting in a greater strength of the perforated structure. In the case of an inplane pattern, the perforations as in a horizontal line perpendicular to the effective overburden load, which results in a greater perforated structure strength than for an inline pattern where the perforations are in a. vertical line parallel to the effective overburden load, resulting in lower perforated structure strength. In addition, the spiral pattern produce the greatest distance between each perforations and therefore a stronger perforated structure. The important feature appears to be the interaction between the perforations and it was recorded that failure of an inline pattern did not occur in all of the perforations at the same applied load. This can be considered in terms of a failed region in one perforation redistributing the load further into the rock mass and shielding the adjacent perforations.

Perforation deformation

The results show that the perforation diameter deformed or decreased asymptotically as the load applied increased. The rate of closure decreased as failure approached.

Figure 4 shows the relationship for one perforation, which can be expressed by the following general equation:

$$D_{ave} = D_i - j(\sigma_V) - m \ln(\sigma_V)$$

FIG. 1 PD AT FAILURE FOR VARIOUS LENGTH

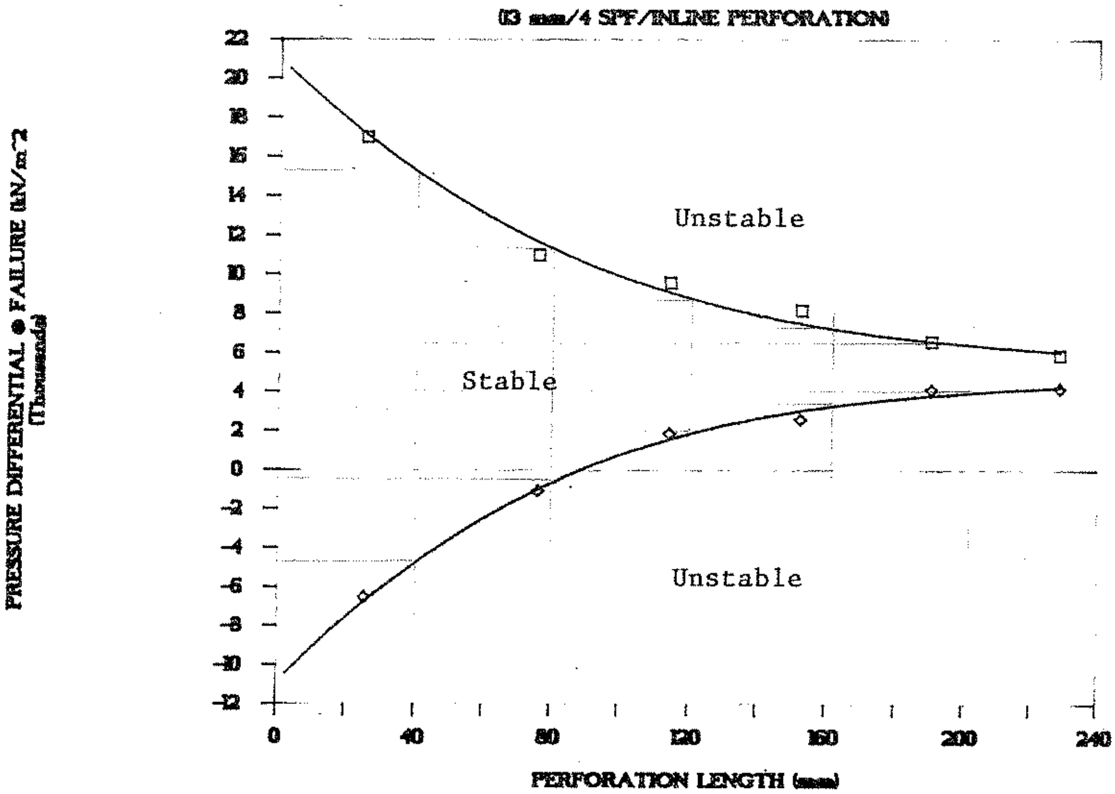

FIG. 2 PD AT FAILURE FOR VARIOUS SHOT DENSITY

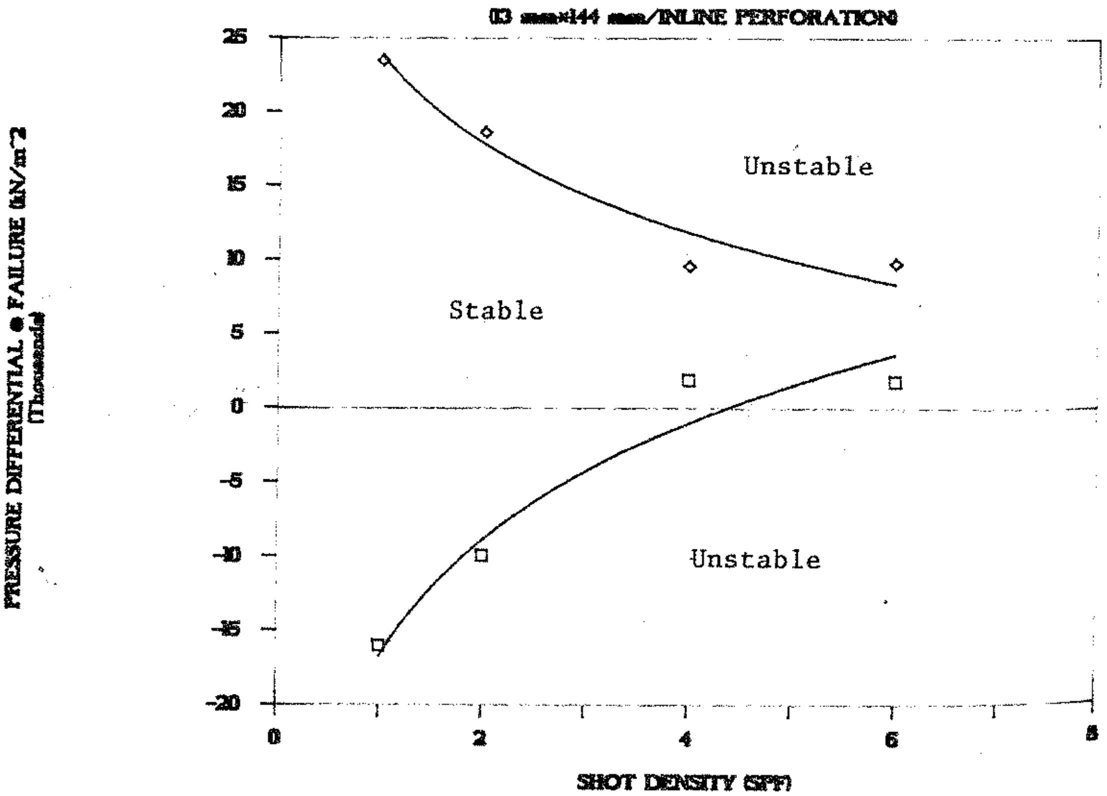

FIG. 3 EFFECT OF PHASING AND PATTERN

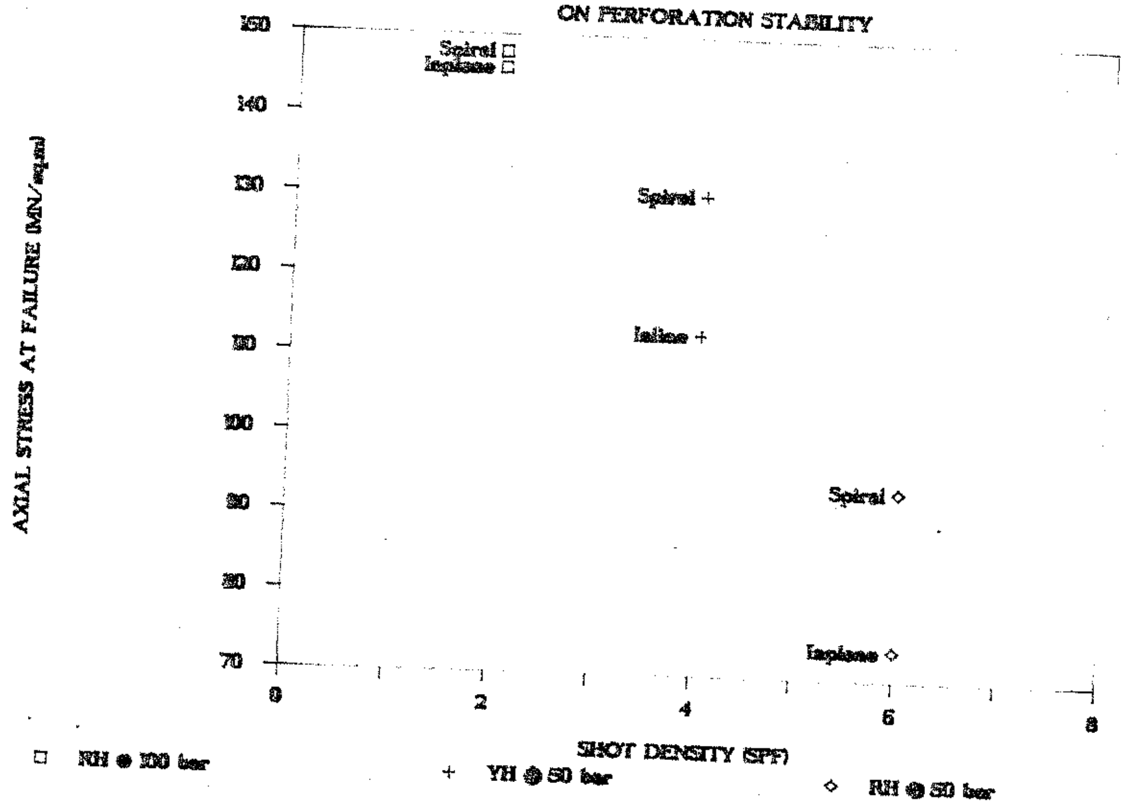

FIG. 4 VERTICAL STRESS VS AVE. PERF. DIAMETER

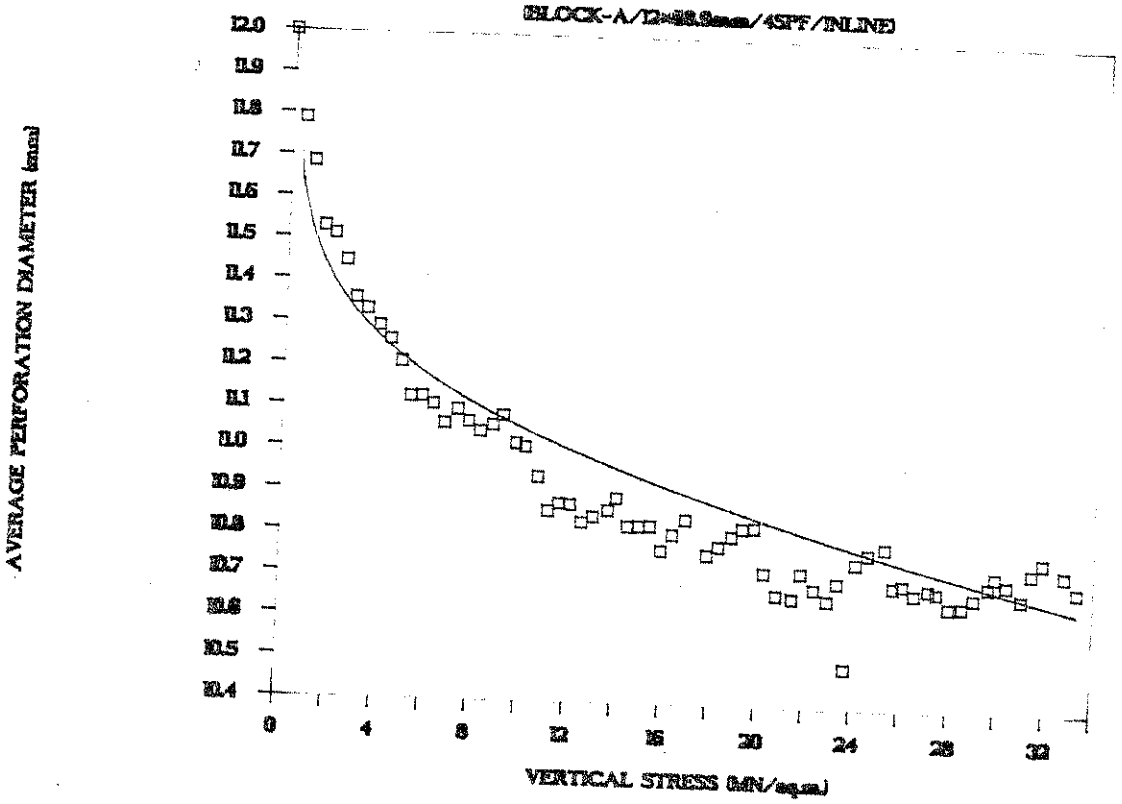

where D_{ave} is the average diameter, D_i is the initial diameter, σ_V is the vertical stress and m and j are factors which depend on the particular geometry of the structure, such as perforation length, shot density, phasing and pattern. The perforation diameter at failure will increase as the perforation length increases and the effect becomes smaller as the shot density increases, since the perforated wellbore stability decreases, therefore the perforation diameter has deformed less (before failure).

The effect of perforation length on perforation deformation also depends on perforation phasing and pattern, as shown in Fig. (5). This is due to the reduced stability of inline perforation pattern compared to that of a spiral pattern, therefore the deformation of perforation before the model actually failed is smaller.

The results also show that increasing the shot density will reduce the perforation deformation at failure, because the perforated wellbore stability decreases as the shot density increases. The effect of shot density on perforation deformation depends on the perforation length; less as the length increases since the stability decreases.

The interaction between the geometry and the stress dictates the change in perforation diameter. For the most part, the deformation was the result of elastic strain which was relieved if some other part of the structure failed. The spiral patterns showed the greatest reduction in perforation diameter in the elastic structure, since the spiral pattern is the most stable structure or geometry.

Mode and Orientation of Fracture

The orientation and direction of the fractures which developed were complex. The perforation tunnels were seen to fracture at the sides, initiated at the cement-rock interface. The fractures grew along the perforation tunnels as the load was increased, either by direct application of load or by interaction between the perforation and the wellbore. They resemble wellbore break out fractures.

The orientation of fracture around the perforated wellbore, length of fracture along the perforation tunnel and degree of failure depend on the perforation length, shot density, phasing and pattern, confining pressure and structure of the rock mass. The number of fracture generally increases as the shot density increases.

The interaction between the wellbore and the perforations generated break out fractures on the surface of the wellbore, extending from perforation to perforation and produced conical shear fractures around the wellbore. The fracture around the interface between rock-cement is always larger than the surrounding area on the wellbore wall, since it is the critical area: i.e., the area with the highest maximum shear stress. The fractures were of variable length and ranged from 3.15 mm to 22.10 mm in width, the depth ranged from 0.06 mm to 8.10 mm.

In general, there appeared to be 2 distinct modes of deformation. That which occured below the failure load and that which occured during and after failure.

Below the failure load of the structure, there were local fractures created at the sides of the perforation tunnels and at the perforation entrance hole adjacent

FIG. 5 EFFECT OF PERFORATION LENGTH ON

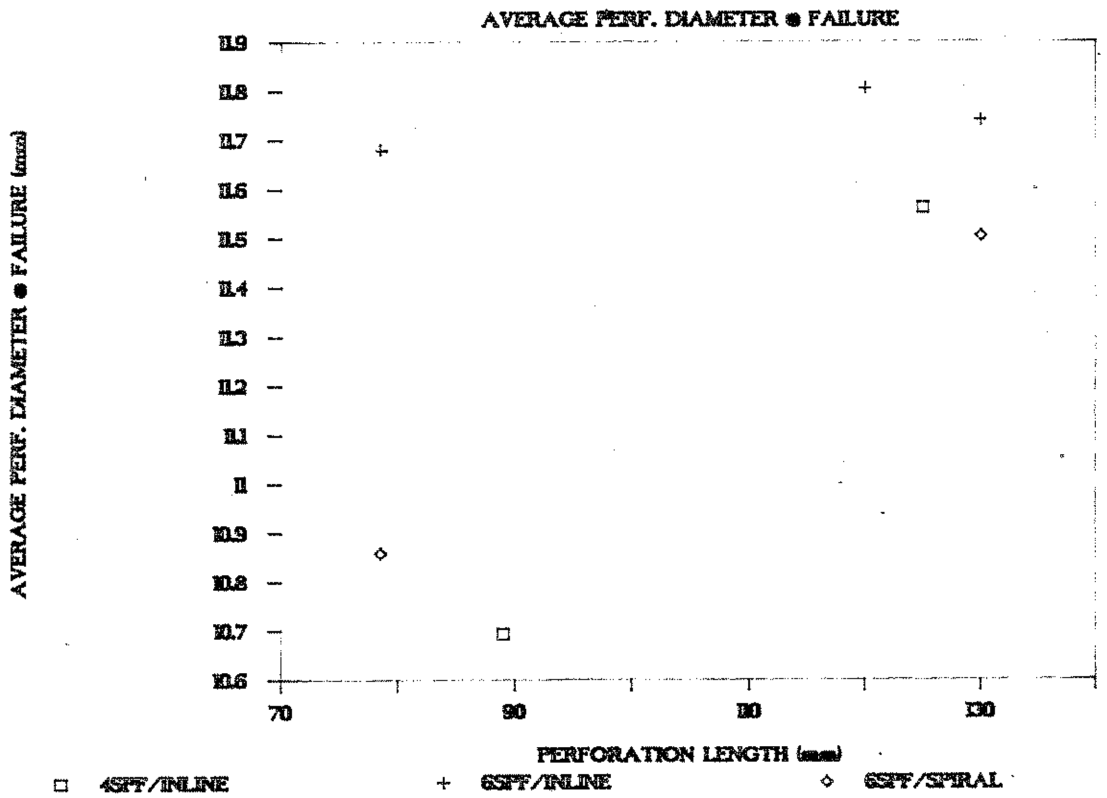

FIG. 6 RECOVERED WEIGHT VS GRAIN SIZE

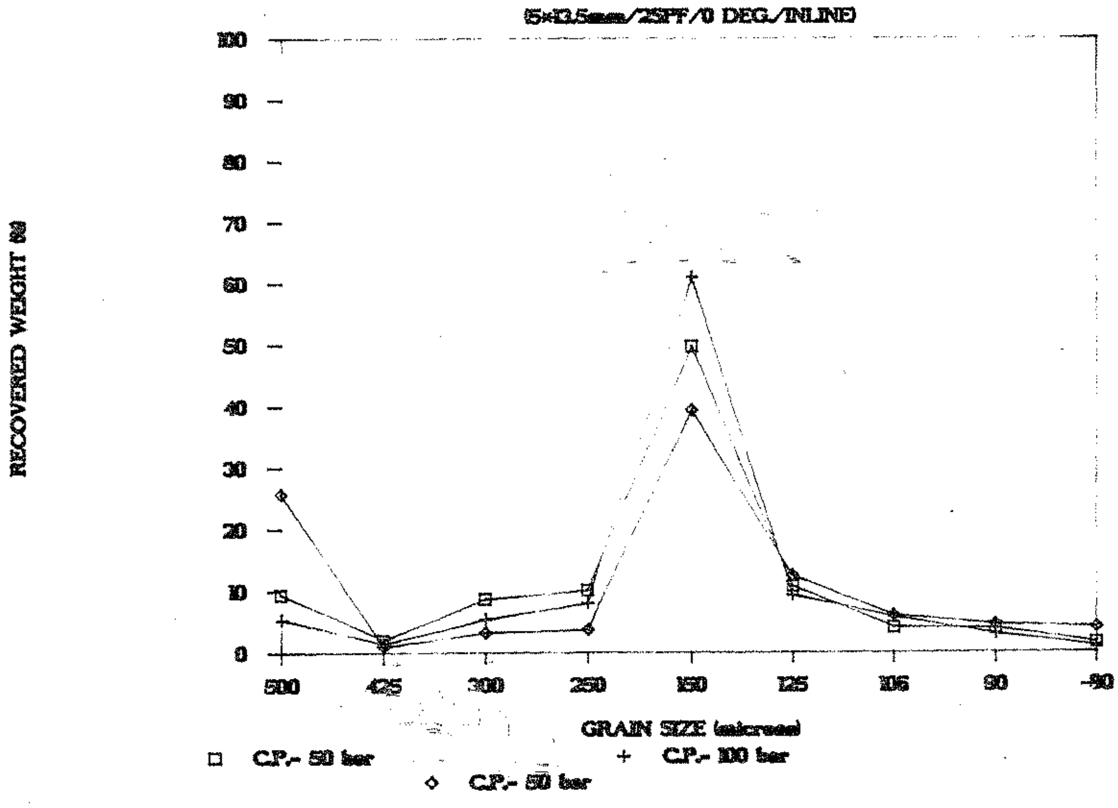

to the wellbore. The extent of these fractures appears to be related to the magnitude and location of the redistributed stresses. The fractures appear to grow only during an increase in the applied stress. These conditions generate the greatest reduction in perforation diameter.

The length of the perforations, the shot density, shot phasing angle and shot pattern also affect the fractures produced.

Amount and Size of Fragments Produced

The debris produced was sieved and produced a normal size distribution for the sandstone tested. The amount of debris was related to the fractures produced and the stability of the structure. The big portion of debris are larger than 500 microns: ranging from 27.08 % to 81.35 % of recovered weight, as shown in Fig. (6).

The debris produced at failure generally increases as the perforation length and shot density increases, and decreases as the phasing angle and changing perforation pattern from inline to inplane and/or spiral, and the confining pressure increase since the perforated wellbore stability decreases. It is significant that increasing the shot density by a factor of 2 will increased the debris produced by a factor of 8.

The debris produced also related to the gross deformation. More stable structure produce less debris. The debris created within the rock adjacent to the perforation tunnel surface will contribute to any possible formation and perforation plugging.

CONCLUSIONS

The study has shown that the deformation of a perforated wellbore due to applied rock stresses is complex. Failure to consider the structural stability as an integral part of the perforated wellbore design may lead to lower than expected productivities, and attribute the cause to some other aspect of the operation.

Consideration must be given to the interaction between the perforations and the wellbore. The results show the formation of fractures within the perforation at loads below the failure load of the rock mass or below the loads which cause wellbore stability problems.

Within the perforations, local failure is initiated at the entrance hole of the perforation or at the cement-rock interface and is extended as shear fractures along the sides of the perforation tunnel as the applied load is increased.

The fractures on the wellbore are initiated at the perforation entrance holes and extending from perforation to perforation around the wellbore wall.

The deformation and failure loads of the structure depend on the material properties and the structural properties such as perforation length, shot density, phasing angle and pattern. In general, the geometry of the individual perforations influences the stability less than the geometry of the structure, that is the shot density, shot phasing angle and pattern. A spiral pattern is the most stable with inplane and inline patterns becoming less stable, respectively.

The shot density produced the most significant results. An increase in shot density reduced the stability and produced a disproportionately large increase in debris. The creation of debris is significant in that it may be mobilised and block the fracture surfaces.

REFERENCES

1. Saucier, R.J. & Land, J.F.: "A laboratory study of perforation in stressed formation rocks". Well Completion 5a, vol. 1, SPE reprint series, 1980.
2. King, G.E., Bingham, M.D. & Kidder, R.W.: "Factors affecting perforating charge performance and relationship to port plug condition". SPE Production Engineering, Sept., 1986.
3. Halleck, P.M., Saucier, R.J., Behrmann, L.A. & Ahrens, T.: "Reduction of jet perforator penetration in rock under stress". SPE paper 18245 in procs. 63rd. Annual Technical Conference and Exhibition SPE-AIME, 1988.
4. Bell, W.T.& Shore, J.B.: "Casing damage from gun perforator". Well Completion 5a, vol. 1, SPE reprint series, 1980.
5. Pattillo, P.D. & Smith, M.B.: "A finite element analysis of collapse of perforated casing". Application of Nonlinear Analysis to Structural Problems, ASME PUP-76, 1983.
6. Bonomo, J.M. & Young, W.S.: "Analysis and evaluation of perforating and perforation cleanup methods". SPE paper 12106 in procs. 58th Annual Technical Conference and Exhibition SPE-AIME, 1983.
7. Aaron Cheng, M.C.: "Perforating damage and shot density analysed". Oil and Gas Journal, March, 1985.
8. Halleck, P.M. & Deo, M.: "The effects of underbalance on perforation flow". SPE paper 16895 in procs. 62nd. Annual Technical Conference and Exhibition SPE-AIME, 1987.
9. Regalbuto, J.A. & Riggs, R.S.: "Underbalanced perforation characteristics as affected by differential pressure". SPE Production Engineering, Feb., 1988.
10. Harris, H.M.: "The effect of perforating on well productivity". JPT, April, 1966. 11. Bell, W.T., Brieger, E.F. & Harrigan, J.W.: "Laboratory flow characteristics of gun perforations". Well Completion 5a, vol. 1, SPE reprint series, 1980.
12. Hong, K.C.: "Productivity of perforated completion in formation with or without damage". JPT, Aug., 1975.
13. Locke, S.: "An advanced method for predicting the productivity ratio of a perforated well". JPT, Sept., 1981.
14. Tariq, S.M.: "Evaluation of flow characteristics of perforations including nonlinear effects with the finite element method". SPE Production Engineering, May, 1987. 15. Tariq, S.M., Ichara, M.J. & Ayestaran, L.: "Performance of perforated completions in the presence of

common heterogeneities:- anisotropy, laminations or natural fractures". SPE paper 14320 in procs 56th. Annual Technical Conference and Exhibition SPE-AIME, 1981.

16. Deo, M., Tariq, S.M. & Halleck, P.M.: "Linear and radial flow targets for characterising downhole flow in perforations". SPE paper 16896 in procs 62nd Annual Technical Conference and Exhibition SPE-AIME, 1987.
17. Stewart, G.: "Modelling of perforation flow performance". SPE Aberdeen Section Continuing Education Seminar, 1987.
18. Vriegen, P.B., Spijker, A. & van der Vlis, A.C.: "Erosion of perforation tunnels in gas wells". SPE paper 5661 in procs 50th Annual Technical Conference and Exhibition SPE-AIME, 1975.
19. Antheunis, D., Vriezen, P.B., Schipper, B.A. & van der Vliss, A.C.: "Perforation collapse:- failure of perforated friable sandstones". SPE paper 5750 in procs. 51st. Annual Technical Conference and Exhibition SPE-AIME, 1976.
20. Morita, N., Whitfill, D.L., Feddle, O.P. & Lovik, T.H.: "Parametric study of sand production prediction:- analytical approach". SPE Production Engineering, Feb., 1989.
21. Morita, N., Whitfill, D.L., Massie, I. & Knudsen, T.W.: "Realistic sand production prediction:- numerical approach". SPE Production Engineering, Feb., 1989.